Int J Physiol Pathophysiol Pharmacol 2021;13(3):94-101
www.ijppp.org /ISSN:1944-8171/IJPPP0121674

Original Article

The change of intracellular zinc distribution after strong acid challenge

Yuli Hu, Yang V Li

Molecular & Cellular Biology Graduate Program, Departments of Biological Sciences and Biomedical Sciences, Ohio University, Athens, OH 45701, USA

Received September 3, 2020; Accepted October 18, 2020; Epub June 15, 2021; Published June 30, 2021

Abstract: Zinc (Zn^{2+}) is stored in the nucleus, endoplasmic reticulum (ER), Golgi apparatus, mitochondria, lysosomes, and zinc-binding proteins. The acidity of the microenvironment affects the binding between zinc and proteins in which zinc become free or loosely bound. In this study, when cells were treated with an acidic medium, we started seeing free zinc 'hot spots' or zincosomes where we found bright zinc fluorescence. The rising free zinc quickly across whole cells with both intensity and distribution were pH-dependent. Interestingly, the nucleus was more sensitive to acidic treatment as the increase of nuclear zinc was faster and higher than the increase of cytosolic zinc. In addition, we re-cultured strong acid-challenged cells in a normal medium. Comparing to the control, these cells exhibited multiple zinc 'hot spots' beside the nucleus, suggesting that free zinc became more extensively distributed. To investigate further the function of zinc in cell shaping and morphological changes, we categorized strong acid-challenged cells into different shapes and found that the proportion of each cell shape had changed after the acid challenge. These acid-induced changes of the cell shape percentage were partially reversed by the reduction of zinc, suggesting that zinc participated in directing the cell shapes and morphologies during cell growth. Our findings reveal that acidic pH affects the dynamics of cellular zinc by making zinc more accessible to cellular compartments and zinc-binding proteins, which provided new insights into understanding the cellular behavior and the function of zinc in it.

Keywords: Zinc, acid, acidity, organelles, pH

Introduction

A correct pH of each cellular compartment is important for the optimal function of enzymes. Cellular acidification affects enzyme activities intracellularly [1-4]. Protein degradation occurs biologically during cellular acidification accompanied by loss-of-function of the enzymes. On the other hand, a decreased pH activates enzymes, such as acid hydrolases, that prefer low pH as the working environment [5, 6]. Cellular acidification occurs during many pathophysiological events, such as inflammation, Alzheimer's disease, ischemia, and cancer [3, 7-10]. To investigate the effect of cellular acidification on cell behavior, we employed acidic treatments to induce changes in cells, especially the change of intracellular zinc distribution.

Zinc (Zn^{2+}) is a trace element needed by the human body for good bone health and immune system [11-14]. It is incorporated into the structures of DNA and proteins for their basic functions [15, 16]. The intracellular distribution of zinc has been reported to be at the nucleus, ER, Golgi apparatus, mitochondria, and lysosomes [17, 18]. The levels of zinc in these zinc-storing compartments are stringently regulated by zinc transporters located on the cell membrane and organelle membrane [11, 19-21]. Zinc-protein binding is tight under basic environment and becomes loosely bound under acidic environment [22]. In response to cellular acidification, stored zinc is released from zinc-storing compartments and zinc-binding proteins to experience new depositions [23, 24]. Here, we report the difference in zinc distribution before and after the strong acid challenge.

In this study, we first used different acidic pH to stimulate zinc increase from zinc-storing compartments and zinc-binding proteins. As a result, zinc increase was observed in the ER, nucleus, and the entire cytosol. The more aci-

dic the pH treatment was, the quicker zinc increase occurred, and the higher zinc level was observed, suggesting that the release of intracellular zinc was pH-dependent. We next used strong acidic pH to stimulate the re-distribution of intracellular zinc, and showed the strong acid challenge has changed the distribution of zinc from the tip of cells to the side of cells. In the end, we analyzed the percentage of different cell morphologies after a strong acid challenge. As a result, the pH 3.0-challenged cells presented a percentage of fewer triangle cells, which was compensated by the administration of zinc chelator TPEN. We speculate that strong acid challenge changed the distribution and the availability of zinc, and contributed to the shaping and behavior of cells.

Methods

Cell culture

T-25 flasks were used to maintain regular cell culture of HeLa cells. HeLa cells were maintained in healthy EMEM medium purchased from ATCC (Manassas, VA) and were used between passages ranging from 6 to 14. The incubation chamber used for HeLa cell culture was set with 95% humidity and 5% carbon dioxide at a temperature of 37°C. HeLa cells are easy to maintain in an incubator with a doubling time of approximately 23 hours, and they are epithelial cells, big (20-40 μm), attached to the culture plates for physiological observations [18].

Treatments

All treatments were done using HEPES buffer prepared as previously described [25, 26]. Hydrogen chloride was used to adjust the pH of HEPES buffers to different acidity. The osmolarity of each HEPES buffer was checked using a vapor pressure osmometer and maintained between the range of 270 and 290 mmol/kg. After pH treatments, HeLa cells were washed with 1X Dulbecco's Phosphate-Buffered Saline (DPBS) and then re-cultured in healthy medium for one day. After 24 hours of the re-culture, cells were taken out for zinc fluorescence observations and morphology observations.

Zinc fluorescence staining

For the zinc transient experiments, HeLa cells were loaded with 0.5 μM FluoZin-3, AM dye for 45 min followed by 30 min of de-esterification in a dye-free HEPES buffer at room temperature. For the zinc distribution observations, HeLa cells were loaded with 1 μM FluoZin-3, AM dye for 60 min followed by 30 min of de-esterification in dye-free HEPES buffer at 37°C. For the zinc transient experiments, pH treatments were given at 2 minutes after the Petri dish was set well on the microscope. For the zinc distribution observations, pH 7.0 HEPES buffer was given to the Petri dish before setting the Petri dish on the microscope. All zinc signals of cells were captured with an objective at 40X. The zinc fluorescent intensity of each transient was calculated using the equation $\Delta F=F_{measure}-F_0$. $F_{measure}$ was the intensity read through time, and F_0 was the intensity read at 0 minutes.

Morphology observation

Three groups of HeLa cells were pre-treated with solutions of pH 7.4 with ethanol, pH 7.4 with ethanol, and pH 7.4 with 10 μM TPEN prepared in HEPES buffer for 5 min. Ethanol was the carrier control for TPEN. Then, they were treated with solutions of pH 7.4 with ethanol, pH 3.0 with ethanol, and pH 3.0 with 10 μM TPEN prepared in a HEPES buffer for 10 min. The final ethanol concentration in TPEN or control groups was 0.03%. After treatments, cells were washed with DPBS and re-cultured in the healthy medium for one day. At 24 hours, bright-field images of cells were captured with an objective at 10X. Numbers of each cell shape were counted from the captured images. Cell shape percentage was calculated by dividing the number of each cell shape by the total number of all cell shapes.

Statistics

Means of experiments were calculated, and standard deviations were presented in the figures. Student's *t-tests* were performed in the Microsoft Excel between two groups with the assumption of equal variance. *P* values were calculated to present statistical significances.

Results

HeLa cell line was used for fluorescent microscopic observation due to that it is well attached to the glass-bottom cell plates, big in size, and grows into a single layer with flat cell morphology. We have used HeLa cells to study zinc response and distributions [18]. Zinc is tightly regulated in a healthy cell where labile or free

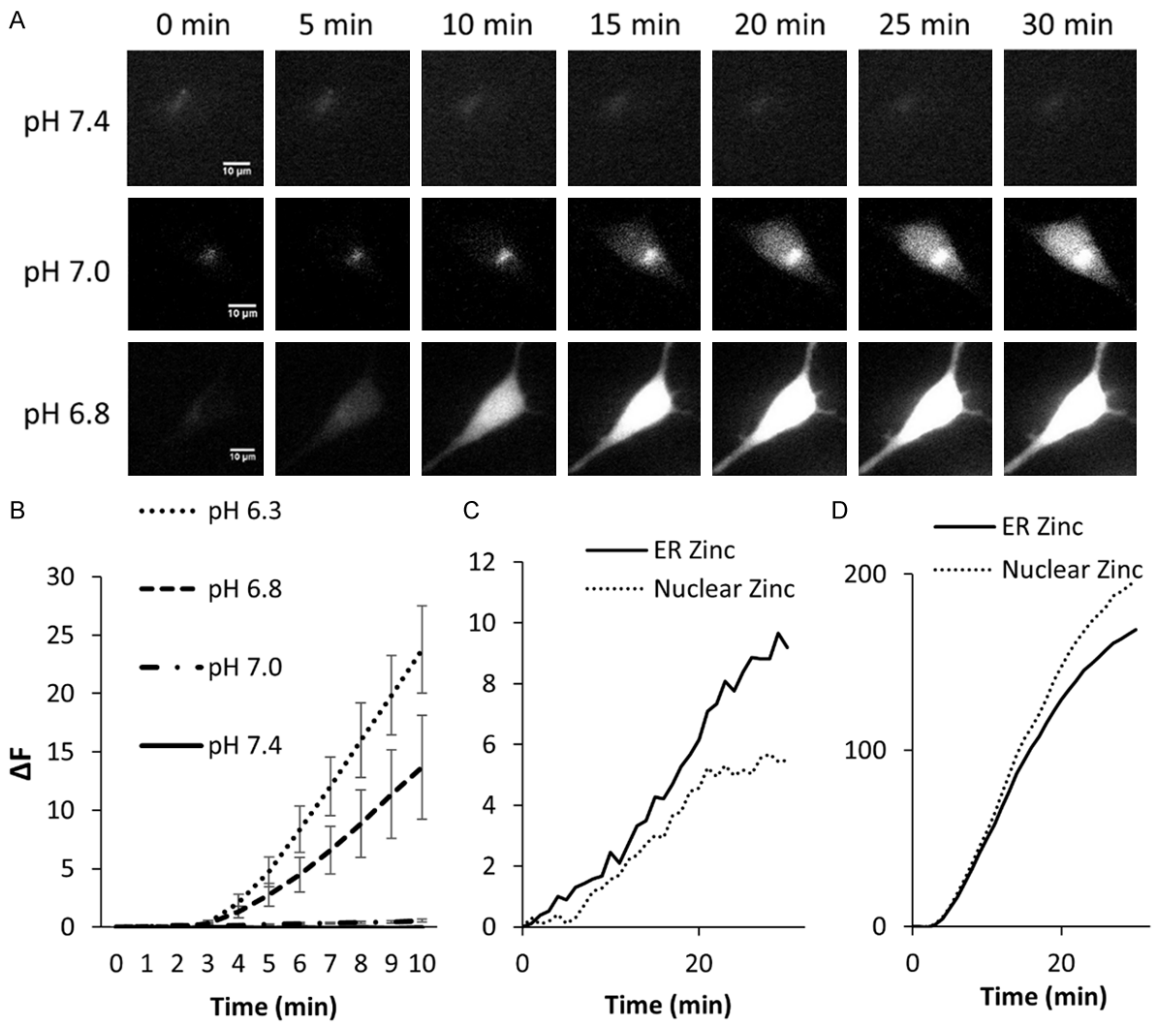

Figure 1. Increases of intracellular free zinc by the acid challenge. HeLa cells were loaded with FluoZin-3, AM (0.5 μM) and placed in pH 7.4 HEPES buffer at 0 minutes, and pH treatments were administrated at 2 minutes and through the recording. (A) Images of intracellular free zinc indicated by zinc fluorescence after pH 7.4, 7.0, and 6.8 treatments. Zinc fluorescence was not changed in pH 7.4. There was a zinc rise in both pH 7.0 and pH 6.8. Images recorded at 0, 5, 10, 15, 20, 25, and 30 minutes are presented. Scale bars were 10 μm. (B) Line graph showing whole-cell zinc increases after pH 7.4, 7.0, 6.8, and 6.3 treatments. Zinc fluorescence of pH 7.4 (3 cells from 3 dishes), pH 7.0 (3 cells from 1 dish), pH 6.8 (3 cells from 1 dish), and pH 6.3 (4 cells from 2 dishes) were recorded every minute between 0-10 minutes. Data represent means ± SD. (C) Line graph showing zinc rises in the ER and nucleus at pH 7.0. (D) Ling graph showing zinc rises in the ER and nucleus at pH 6.8. Data in (C & D) represent the mean of zinc fluorescence from three cells. The y-axis in (B-D) is ΔF.

Zn^{2+} is maintained very low in the cytosol [21, 27]. Therefore, it didn't surprise that zinc was not detectable using fluorescent indicator when cells were treated at normal pH 7.4 (**Figure 1A**). However, we observed dynamic changes and increases in intracellular free zinc by acidic treatments. The treatments of pH 7.0 and pH 6.8 triggered intracellular free zinc increase significantly (**Figure 1A**). The pH 6.8-stimulated whole-cell zinc signal appeared early at 5 minutes compare to that of pH 7.0 group at 15 minutes (**Figure 1A**). The more acidic the treatment was, the faster and higher the zinc signal appeared (**Figure 1B**), suggesting that intracellular zinc increased in a pH-dependent manner. Since zinc rise at pH 7.0 was relatively slow and moderate, it allowed us to note the difference of Zn^{2+} signals at the cytosol organelles and the nuclear region. There was usually a brighter Zn^{2+} signal that was likely in the ER region (**Figure 1A**, pH 7.0), which increased earlier than zinc signal in the nucleus (**Figure 1C**). At

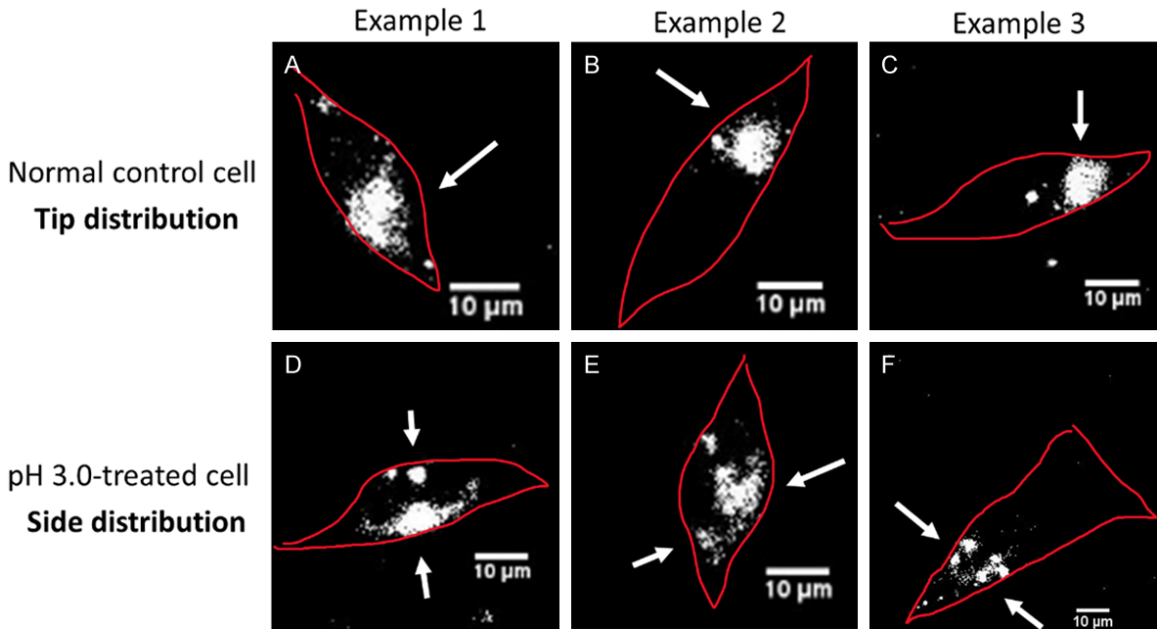

Figure 2. The acid challenge changed the dynamic distribution of zinc (two-dimensional). HeLa cells were challenged with pH 7.4 (sham control) and 3.0 for 10 min, washed with PBS, and re-cultured in a healthy medium for one day. At 24 hours, cells were stained with 1 μM FluoZin-3, AM dye, and observed under a fluorescent microscope. A-C. Examples showing zinc distribution at the tip region of cells after re-culture from pH 7.4 control. D-F. Examples showing zinc distribution at the side of cells after re-culture from the pH 3.0 challenge. Red lines outlined the shapes of each cell. Scale bars =10 μm.

pH 6.8, both nuclear and ER (or the cytosol) gave rapid increases of zinc fluorescence that reached fluorescence saturation (**Figure 1A** and **1D**, pH 6.8), which indicated that the nucleus was also sensitive to acidic treatment.

To investigate the distribution of zinc after acid challenge, in separate tests, cells were treated with brief strong acidic pH 3.0 for 10 min. We collected survived cells and re-cultured them in a normal medium at pH 7.4 for 24 hours. The density of the re-cultured cells was only about 10-30% of cell seeding density prior to strong acidic treatment. After one day of culture, all re-cultured cells appeared normal in the healthy medium with no detectable zinc fluorescence. However, when these cells were placed at pH 7.0 medium for observing the dynamic changes of zinc distribution, we observed different patterns of zinc fluorescence between pH 3.0 challenged cells and controls (We didn't place cells in pH 6.8 or lower medium since cells will be quickly saturated with zinc fluorescence as shown in **Figure 1A**). As shown in **Figure 2**, the zinc distribution of control cells was accumulated at the tip region of cells with one concentrated hot spot of zinc fluorescence (**Figure 2A-C**). The zinc distribution of pH 3.0-treated cells was more dispersed and usually into the side regions of cells (**Figure 2D-F**) with multiple hot spots. By observing these cells for 20 minutes in movies, we studied the dynamic changes of zinc peaks within zinc fluorescence hot spots (**Figure 3**). There was only one stationed zinc peak that stayed in the control (**Figure 3A-E**). There were multiple zinc peaks in the pH-3.0 treated cell (**Figure 3F-J**), suggesting that strong acid challenge changed the dynamic nature of zinc distribution.

To understand better the function of zinc distribution after strong acid challenge, we further categorized the strong acid challenged-cells into different shapes: round, spindle, triangle, and irregular. If a cell did not fit into any of the round, spindle, or triangle shapes, this cell was recognized as an irregular cell. HeLa cells were treated with pH 7.4 (sham control), pH 3.0, and pH 3.0 with TPEN respectively, and then survived cells were re-cultured in a healthy medium for 24 hours. We found that the pH 3.0 challenge increased the percentage of spindle cells by 17% and reduced the percentage of triangle cells by 22%. TPEN was used to reduce the effect of acid-stimulated intracellular zinc. Compared to the pH 3.0-treated group, pH 3.0

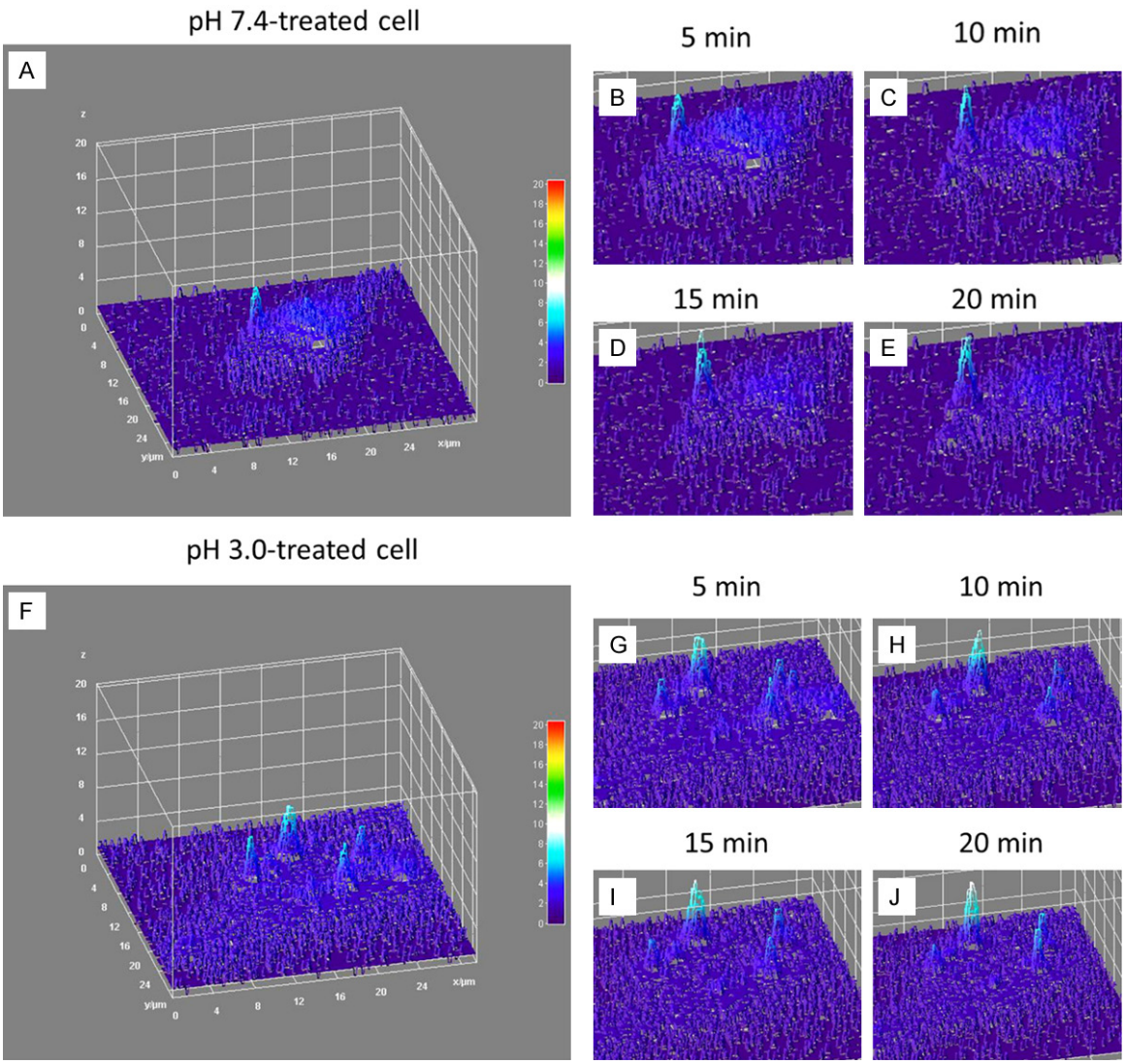

Figure 3. Acid challenge affected the dynamic nature of zinc peak (three-dimensional). HeLa cells were challenged with pH 7.4 and 3.0 for 10 min, washed with PBS, and re-cultured in a healthy medium for one day. At 24 hours, cells were stained with 1 μM FluoZin-3, AM dye, and observed under a fluorescent microscope. A & F. Showing one zinc-peak distribution from a pH 7.4 control cell, and multiple zinc-peak distributions from a pH 3.0-treated cell during observations of 20 minutes. Images stacked for the movies were obtained every minute. B-E & G-J. Representative images of zinc peaks cropped from each movie at 5, 10, 15, and 20 minutes.

treatment with TPEN reduced the percentage of round cells by 4% and compensated the percentage of triangle cells by 12%, suggesting that zinc might participate in directing the morphology of cells.

Discussion

Here, we report a new phenomenon of cellular zinc distribution after strong acid challenge with the following main findings: (1) Treating cells with acidic medium stimulates increases of zinc from zinc-storing compartments and zinc-binding proteins, quickly rising in organelles, nucleus, and the entire cytosol. The more acidic the pH treatment was, the quicker zinc increase occurred, and the higher zinc level was observed, suggesting that the release of intracellular zinc was pH-dependent. (2) We discover that acidic treatment stimulates zinc re-distribution. Strong acidic challenged cells gave rise to increased zinc hotspot or zinco-somes. (3) We also discover that cell shapes are affected by acidic treatment, which are also sensitive to the presence of zinc, suggesting that altered zinc dynamic may participate in directing morphology and behavior of cells.

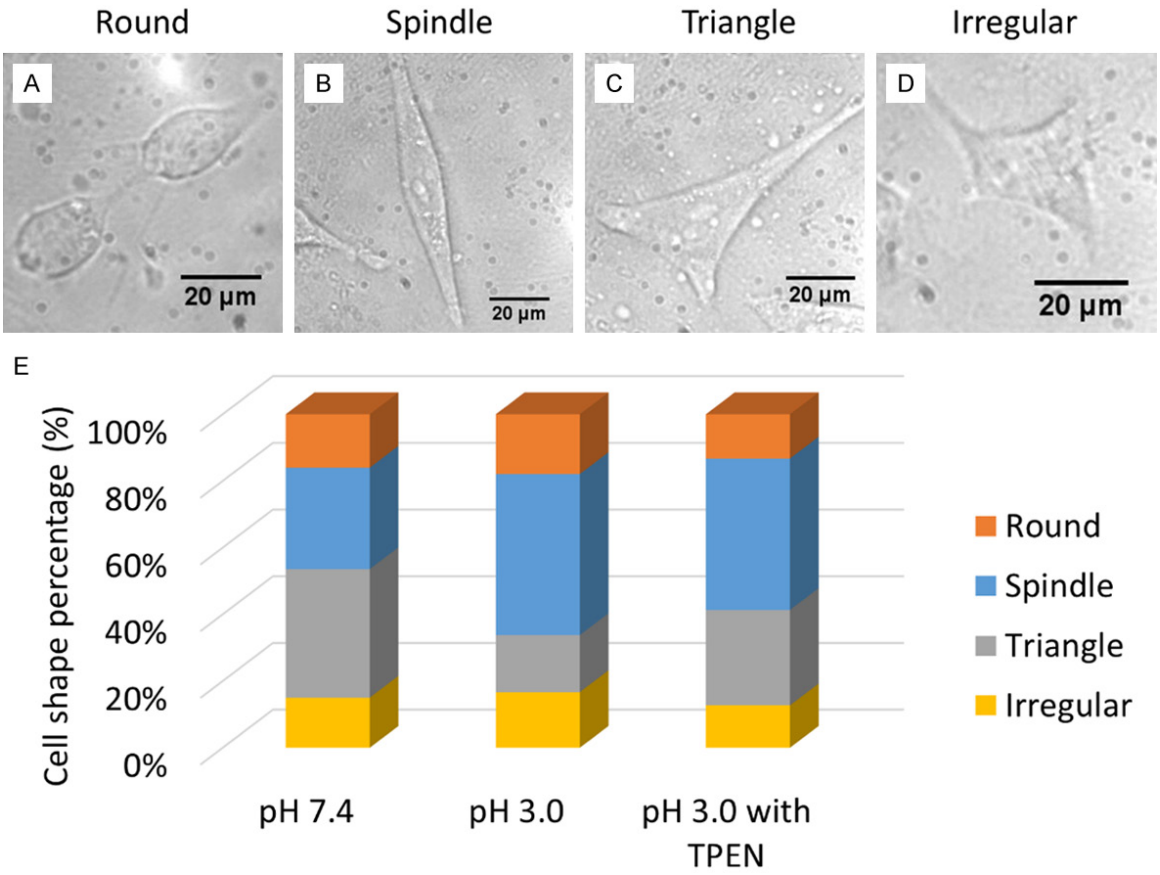

Figure 4. The acid challenge changed the percentage of different cell shapes. A-D. Example images showing cell shapes of round, spindle, triangle, and irregular. Cells that did not fit round, spindle, or triangle shapes were defined as irregular cells. Scale bars =20 μm. E. HeLa cells were treated with pH 7.4, pH 3.0, and pH 3.0 with 10 μM TPEN for 10 minutes with pre-treatments at pH 7.4 with or without TPEN for 5 minutes. All treatments contained 0.03% ethanol because ethanol was used to dissolve TPEN. After treatments, cells were washed with PBS and re-cultured in a healthy medium for one day. At 24 hours, numbers of each cell shape were counted. Cell shape percentage was calculated by dividing the number of a cell shape by the total number of all cell shapes. Data represent the means of 3 experiments for each group.

The pH values of cellular compartments are different for organelle and enzyme functions [1-6]. For example, the cytosol of a cell has a pH of about pH 7.2. In the secretory pathway, the pH of ER is 7.2, and the pH of Golgi apparatus is from 6.0 (*trans*-Golgi) to 6.7 (*cis*-Golgi). The mitochondrial matrix has a more alkaline pH at about pH 8, as mitochondria undergo spontaneous depolarization. Regulators such as sodium (Na^+)-H^+ exchangers (NHEs), Na^+-HCO_3^- co-transporters, anion exchangers, and plasma membrane Calcium-ATPases play roles in maintaining cellular pH [4, 28-30]. Membrane diffusion also allows movements of protons (H^+) from the cytosol to extracellular space and vice versa depending on the concentration gradient of H^+ [31-34], which contributed to rapid zinc dissociation from their binding protein due to H^+ influx (**Figure 1**). The nuclear pH is to be the same as the cytosol due to the abundance of nuclear pores on the nucleus membrane allowing diffusion of H^+ into the nucleus [28, 30, 35], which is the reason that we observed the rapid rising zinc fluorescence in the nucleus.

Zinc bind with proteins as structure, functional, and enzymatic motifs/domains [36]. A protein/enzyme generally has optimum activity over the narrow pH range in which a molecule exists in its properly charge form. Therefore, proteins/enzymes are sensitive to changes in H^+ concentration or pH. Any change in pH, even a small one, alters the degree of ionization of an enzyme's acidic and basic side groups and the substrate components as well. Zinc binding

with protein is pH dependent, which is reversible dissociated in acidic pH [22, 37]. Acidic stimulation favors the dissociation of bound-zinc from zinc-binding proteins, so that these zinc ions become available for fluorescent imaging. When cells are placed in pH 7.4 solution, very few free-zinc could be visualized after zinc fluorescent staining (**Figure 1A**). When cells were placed in acidic solution, zinc fluorescence was visible in the area surrounding the nucleus. Furthermore, in the cells that survived pH 3.0 stimulation, the distribution of zinc changed to become more spread out (**Figures 2** and **3**), which may indicate the increased activity of zinc-binding protein/enzymes in certain cellular regions, and may be contributing to the shaping and behavior of cells (**Figure 4**).

The morphologies of cells were categorized as one of four types: spindle, round, triangle, and irregular shapes [38, 39]. Spindle cells with elongated shapes were cells at the G1 cell cycle, which have better mobility across membranes due to their thin shaping [40]. Triangle cells were cells at the S phase for DNA synthesis [38, 39]. The pH 3.0-challenged cells showed more spindle cell accumulation (or prolonged G1) and fewer triangle cells. The round cell is implied undergoing mitosis as cells need to acquire a round shape to provide space for the mitotic spindle [39]. The reduction of zinc using TPEN reduced the percentage of round cells and increased (reversed) the percentage of triangle cells (**Figure 4E**). Therefore, zinc may play a role in the cell cycle of survived cells from the brief strong acid treatment. A sudden change of pH to extreme acidity may occur under pathophysiological conditions, such as gastric ulcer or gastric cancer. The lesion of the gastric ulcer is exposed to very low acidic pH, so that strong acid contacts with epithelial cells of the stomach. Our results suggest that the contact may result in the changes in cell growth such as the accumulation of spindle cells 24 h after acid treatment. The possible long-term effects of acid-cell interaction will need to be assessed further.

Disclosure of conflict of interest

None.

Address correspondence to: Dr. Yang V Li, Department of Biomedical Sciences, Ohio University, Heritage College of Osteopathic Medicine, 346 Irvine Hall, Athens, OH 45701, USA. Tel: 740-593-2384; Fax: 740-593-2778; E-mail: liy1@ohio.edu

References

[1] Whitten ST, Wooll JO, Razeghifard R, Garcia-Moreno B and Hilser VJ. The origin of pH-dependent changes in m-values for the denaturant-induced unfolding of proteins. J Mol Biol 2001; 309: 1165-1175.

[2] Shan B, Bhattacharya S, Eliezer D and Raleigh DP. The low-pH unfolded state of the C-terminal domain of the ribosomal protein L9 contains significant secondary structure in the absence of denaturant but is no more compact than the low-pH urea unfolded state. Biochemistry 2008; 47: 9565-9573.

[3] Silberman A, Goldman O, Boukobza Assayag O, Jacob A, Rabinovich S, Adler L, Lee JS, Keshet R, Sarver A, Frug J, Stettner N, Galai S, Persi E, Halpern KB, Zaltsman-Amir Y, Pode-Shakked B, Eilam R, Anikster Y, Nagamani SCS, Ulitsky I, Ruppin E and Erez A. Acid-induced downregulation of ASS1 contributes to the maintenance of intracellular pH in cancer. Cancer Res 2019; 79: 518-533.

[4] Yang OCY and Loh SH. Acidic stress triggers sodium-coupled bicarbonate transport and promotes survival in A375 human melanoma cells. Sci Rep 2019; 9: 6858.

[5] Shriver JW. Protein structure, stability, and interactions. New York, N.Y.: Humana; 2009.

[6] Konermann L. Protein unfolding and denaturants. Chichester, UK: John Wiley & Sons, Ltd; 2012.

[7] Webb BA, Chimenti M, Jacobson MP and Barber DL. Dysregulated pH: a perfect storm for cancer progression. Nat Rev Cancer 2011; 11: 671-677.

[8] Mena HA, Zubiry PR, Dizier B, Schattner M, Boisson-Vidal C and Negrotto S. Acidic preconditioning of endothelial colony-forming cells (ECFC) promote vasculogenesis under proinflammatory and high glucose conditions in vitro and in vivo. Stem Cell Res Ther 2018; 9: 120.

[9] Wolfe DM, Lee JH, Kumar A, Lee S, Orenstein SJ and Nixon RA. Autophagy failure in Alzheimer's disease and the role of defective lysosomal acidification. Eur J Neurosci 2013; 37: 1949-1961.

[10] Gores GJ, Nieminen AL, Wray BE, Herman B and Lemasters JJ. Intracellular pH during "chemical hypoxia" in cultured rat hepatocytes. Protection by intracellular acidosis against the onset of cell death. J Clin Invest 1989; 83: 386-396.

[11] Levaot N and Hershfinkel M. How cellular Zn(2+) signaling drives physiological functions. Cell Calcium 2018; 75: 53-63.

[12] Haase H and Rink L. Functional significance of zinc-related signaling pathways in immune cells. Annu Rev Nutr 2009; 29: 133-152.
[13] Rink L and Gabriel P. Zinc and the immune system. Proc Nutr Soc 2000; 59: 541-552.
[14] Fukada T, Yamasaki S, Nishida K, Murakami M and Hirano T. Zinc homeostasis and signaling in health and diseases: zinc signaling. J Biol Inorg Chem 2011; 16: 1123-1134.
[15] Dreosti IE. Zinc and the gene. Mutat Res 2001; 475: 161-167.
[16] Hu Y and Li YV. Expression of SSEA-4 and Oct-4 from somatic cells in primary mouse gastric cell culture induced by brief strong acid. Mol Cell Biochem 2021; [Epub ahead of print].
[17] Stork CJ and Li YV. Zinc release from thapsigargin/IP3-sensitive stores in cultured cortical neurons. J Mol Signal 2010; 5: 5.
[18] Lu Q, Haragopal H, Slepchenko KG, Stork C and Li YV. Intracellular zinc distribution in mitochondria, ER and the Golgi apparatus. Int J Physiol Pathophysiol Pharmacol 2016; 8: 35-43.
[19] Kambe T, Yamaguchi-Iwai Y, Sasaki R and Nagao M. Overview of mammalian zinc transporters. Cell Mol Life Sci 2004; 61: 49-68.
[20] Eide DJ. Zinc transporters and the cellular trafficking of zinc. Biochim Biophys Acta 2006; 1763: 711-722.
[21] Li YV. Zinc overload in stroke. In: Li YV, Zhang JH, editors. Metal Ion in Stroke. 1st edition. New York: Springer Science+Business Media; 2012. pp. 167-189.
[22] Krezel A and Maret W. The biological inorganic chemistry of zinc ions. Arch Biochem Biophys 2016; 611: 3-19.
[23] Kiedrowski L. Cytosolic acidification and intracellular zinc release in hippocampal neurons. J Neurochem 2012; 121: 438-450.
[24] Qiao W, Ellis C, Steffen J, Wu CY and Eide DJ. Zinc status and vacuolar zinc transporters control alkaline phosphatase accumulation and activity in Saccharomyces cerevisiae. Mol Microbiol 2009; 72: 320-334.
[25] Slepchenko KG, Lu Q and Li YV. Zinc wave during the treatment of hypoxia is required for initial reactive oxygen species activation in mitochondria. Int J Physiol Pathophysiol Pharmacol 2016; 8: 44-51.
[26] Slepchenko KG, Lu Q and Li YV. Cross talk between increased intracellular zinc (Zn(2+)) and accumulation of reactive oxygen species in chemical ischemia. Am J Physiol Cell Physiol 2017; 313: C448-C459.
[27] Li Y and Maret W. Transient fluctuations of intracellular zinc ions in cell proliferation. Exp Cell Res 2009; 315: 2463-2470.
[28] Paulino C and Kuhlbrandt W. pH- and sodium-induced changes in a sodium/proton antiporter. Elife 2014; 3: e01412.
[29] Putney LK and Barber DL. Na-H exchange-dependent increase in intracellular pH times G2/M entry and transition. J Biol Chem 2003; 278: 44645-44649.
[30] Ruprecht V, Monzo P, Ravasio A, Yue Z, Makhija E, Strale PO, Gauthier N, Shivashankar GV, Studer V, Albiges-Rizo C and Viasnoff V. How cells respond to environmental cues - insights from bio-functionalized substrates. J Cell Sci 2017; 130: 51-61.
[31] Gutman M, Nachliel E and Moshiach S. Dynamics of proton diffusion within the hydration layer of phospholipid membrane. Biochemistry 1989; 28: 2936-2940.
[32] Reshkin SJ, Greco MR and Cardone RA. Role of pHi, and proton transporters in oncogene-driven neoplastic transformation. Philos Trans R Soc Lond B Biol Sci 2014; 369: 20130100.
[33] Polle A and Junge W. Proton diffusion along the membrane surface of thylakoids is not enhanced over that in bulk water. Biophys J 1989; 56: 27-31.
[34] Casey JR, Grinstein S and Orlowski J. Sensors and regulators of intracellular pH. Nat Rev Mol Cell Biol 2010; 11: 50-61.
[35] Seksek O and Bolard J. Nuclear pH gradient in mammalian cells revealed by laser microspectrofluorimetry. J Cell Sci 1996; 109: 257-262.
[36] Maret W. Zinc biochemistry: from a single zinc enzyme to a key element of life. Adv Nutr 2013; 4: 82-91.
[37] Pantoliano MW, Valentine JS, Burger AR and Lippard SJ. A pH-dependent superoxide dismutase activity for zinc-free bovine erythrocuprein. Reexamination of the role of zinc in the holoprotein. J Inorg Biochem 1982; 17: 325-341.
[38] Bongiorno T, Gura J, Talwar P, Chambers D, Young KM, Arafat D, Wang G, Jackson-Holmes EL, Qiu P, McDevitt TC and Sulchek T. Biophysical subsets of embryonic stem cells display distinct phenotypic and morphological signatures. PLoS One 2018; 13: e0192631.
[39] Cadart C, Zlotek-Zlotkiewicz E, Le Berre M, Piel M and Matthews HK. Exploring the function of cell shape and size during mitosis. Dev Cell 2014; 29: 159-169.
[40] Santamaria PG, Mazon MJ, Eraso P and Portillo F. UPR: an upstream signal to EMT induction in cancer. J Clin Med 2019; 8: 624.